Design Of Multi-mode Switching And Safety Protection System For Home Smart Maintenance Beds And Chairs Based On Edge Computing

Xiao Wang[1], Huayang Meng[2*], and Hui Liu[1]

[1] *School of Intelligent Engineering, Taishan College of Science and Technology, Tai'an 271000, China*
[2] *Medical Engineering Department, The Second Affiliated Hospital of Shandong First Medical University, Tai'an 271000, China*
[*] *Corresponding author. E-mails: dream880810@126.com*

Received April 21, 2026; accepted June 2, 2026

To address high cloud delay, large switching impact, lagging safety response, and insufficient hierarchical protection in traditional bed-chair systems, this paper constructs an edge-computing-based home intelligent nursing bed-chair architecture, establishes a kinematic model and trajectory planning for multi-mode switching, and proposes an adaptive fuzzy PID smooth switching control algorithm with a load-adaptive tuning mechanism and synchronization strategy, along with a hierarchical safety decision method using improved fuzzy evaluation. Test results show that across six common modes, maximum angle error is below 0.35°, The peak acceleration is only 0.22 m/s^2, and impact acceleration stays within 0.25 m/s^2. Under edge deployment, average safety response time is 147 ms, protection success rate 99.2%, false alarm rate below 0.8%, and no fault shutdown after 72 hours. The system maintains excellent stability and robustness under varying loads and scenarios, significantly outperforming traditional PID and cloud-based systems. This study provides a feasible technical path for low-latency control and intelligent upgrading of home rehabilitation aids, suitable for home-based elderly care, community healthcare, and home hospital beds.

Keywords: computer network; edge computing; intelligent maintenance bed and chair; multi-mode switching; adaptive fuzzy PID

http://dx.doi.org/10.6180/jase.202610_33.048

1. Introduction

With global population aging accelerating, demand for home care of disabled/semi-disabled elderly is growing, making intelligent bed-chair integrated equipment a research hotspot. Rao et al. [1] built an intelligent monitoring system for wheelchair-bed integration but only achieved basic shape switching and single-dimensional data collection, without optimizing motion smoothness or multi-scene safety. Bai et al. [2] focused on comfort in static bed rest, not dynamic multi-mode switching control. Wang et al. [3] reviewed home intelligent robots for bedridden elderly, identifying poor dynamic adaptability and limited safety mechanisms but offered no practical solutions. Zhang et al. [4] emphasized multi-mode switching and active safety as future breakthroughs yet noted large switching impacts and lagging responses, without developing control algorithms. Nunes et al. [5] developed a wireless monitoring patch for vital signs but lacked closed-loop linkage with motion control. Menon et al. [6] evaluated smart furniture design for hospital beds, not home-based multi-mode control. Kumari et al. [7] created an IoT-based smart seat with only physiological monitoring, no posture adjustment or active safety. Fritz et al. [8] proposed a health event detection system for home care but focused on post-event alarms, not real-time risks. Sarkar et al. [9] developed a deep-learning fiber-optic sensor bed but only optimized sensing, not the full perception-decision-execution loop. Sawyer et al. [10] defined a design framework for multi-mode products but

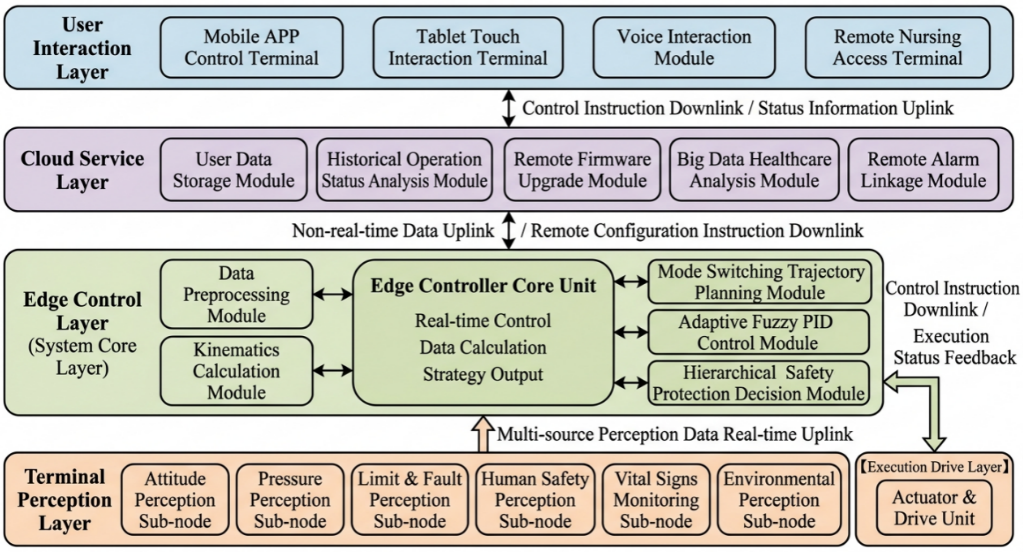

Fig. 1. Overall architecture of household intelligent curing bed and chair system based on edge computing

not customized for home care beds/chairs. Kumar et al. [11] developed an adaptive LPWAN/WiFi edge network for low-latency communication but not for bed-chair real-time control. Recmanik et al. [12] reviewed vital sign sensors for hospital beds without addressing multi-sensor fusion or risk quantification. Mohammed et al. [13] proposed a federated learning-based edge-cloud wheelchair system for outdoor navigation, not home bed-chair switching. Liu et al. [14] developed a proximity/pressure dual-mode sensor but lacked system-level closed-loop control. Pomante and Salice [15] built a monitoring system for sleep and fall detection only in static rest, not dynamic mode switching. Jeung et al. [16] developed an AI-driven hospital bed safety system focused on risk warning, not hierarchical protection execution. Zhang et al. [17] proposed inherent safety design for nuclear plants, which has not yet been applied to home intelligent bed-chair systems.

In summary, current research on intelligent nursing beds and wheelchairs still faces three bottlenecks: lack of smooth trajectory planning and load-adaptive control for bed-chair switching, reliance on cloud-based processing with high latency and offline failure, and single emergency-stop safety mechanisms without hierarchical protection. To address these, this paper proposes an edge-computing-based multi-mode switching and safety protection system. It designs a four-layer perception-edge-control-cloud architecture, establishes a kinematic model with fifth-degree polynomial trajectory planning for impact-free switching, adopts an adaptive fuzzy PID controller for high-precision control, and constructs a graded safety decision model using improved fuzzy comprehensive evaluation for comprehensive risk identification and active protection.

- **Methodological innovation in control algorithm:** Proposed an adaptive fuzzy PID algorithm with a load-adaptive parameter tuning mechanism. This differs from conventional fuzzy PID by introducing real-time load identification and multi-actuator synchronization control, achieving a peak acceleration of only 0.22 m/s^2 and a 75% reduction in angle control error compared to traditional methods.

- **Architectural innovation in edge computing:** Designed a heterogeneous edge computing architecture utilizing an STM32H743 and a Raspberry Pi 4B for real-time control and safety decision-making, achieving a 98% reduction in security protection response time compared to cloud-based architectures.

- **Theoretical innovation in safety protection:** Constructed a three-level hierarchical safety protection model with an improved fuzzy comprehensive evaluation. This introduces the entropy weight method for objective weight optimization and establishes clear trigger thresholds for different risk scenarios.

These innovations represent methodological advancements beyond mere system integration, providing new technical approaches for the field of home intelligent rehabilitation equipment.

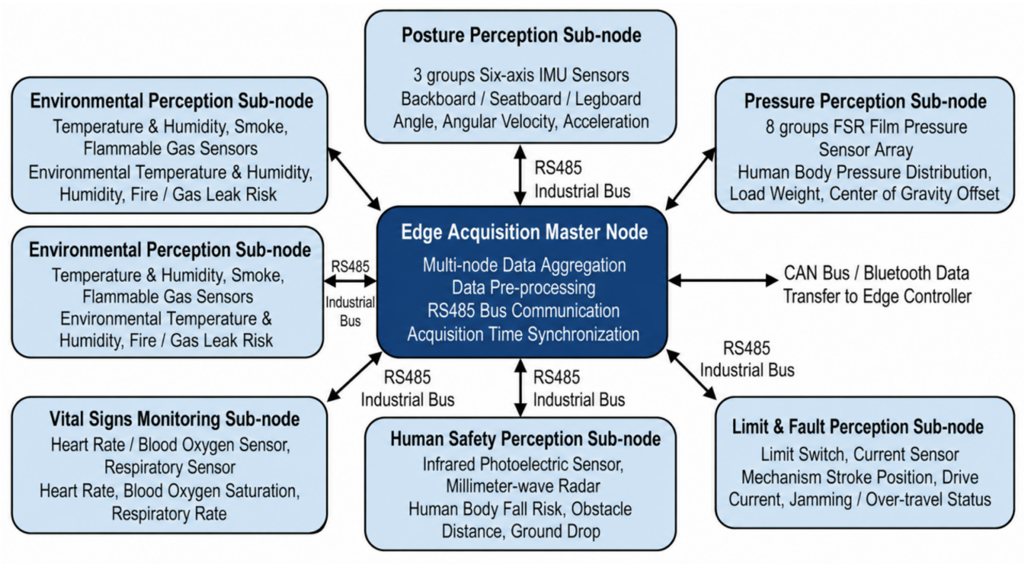

Fig. 2. Multi modal Perception Unit Structure of Intelligent Maintenance Bed and Chair

2. Theory and formula

2.1. Architecture design of intelligent curing bed and chair system based on edge computing

2.1.1. Overall layered architecture of the system

The home intelligent maintenance bed and chair system designed in this article adopts a four layer architecture, including terminal perception layer, edge control layer, cloud service layer, and user interaction layer. The overall structure is shown in Figure 1.

The edge control layer uses STM32H743 for real-time tasks (trajectory planning, fuzzy PID, motor control, safety, interrupts, CAN/RS485/PWM) and Raspberry Pi 4B for preprocessing, fusion, HCI, cloud communication, and monitoring. They communicate via 50 Mbps SPI with 1 s timestamps from STM32. Sensor data is timestamped, sent to Pi for processing, returned to STM32 for control, synchronized within a 1 ms window. Measured latencies: SPI 0.12 ms, preprocessing 1.85 ms, control 3.5 ms, end-to-end below 10 ms.

2.1.2. Multimodal Perception Unit Structure

The multimodal perception unit serves as the system's data foundation for precise mode switching control and active safety decisions, requiring full-dimensional sensing of bed-chair operation status, human posture, and environmental risks. This unit adopts a distributed master-slave node structure [18, 19], as shown in Figure 2.

2.1.3. Multi-mode switching actuator and drive system structure

The system supports six core modes (lying flat, sitting, lifting, leg bending, assisted standing, wheelchair travel), switched via electric push rods and motors [20, 21]. A closed-loop drive structure of edge controller, driver, actuator, and feedback unit is designed for smooth and precise control, as shown in Figure 3.

2.1.4. Hierarchical safety protection closed-loop control structure

To address passive protection and delayed response in traditional bed-chair systems, this paper designs a three-level safety protection system (pre-alarm, active intervention, emergency braking) and constructs a fully closed-loop safety protection control structure [22, 23], as shown in Figure 4.

The system has three safety levels. Level 1 pre-alarm (F 0.25–0.5) handles minor risks like 5–10 cm offset or ±20% heart rate change with yellow light and alert, no motion intervention. Level 2 active intervention (F 0.5–0.75) handles moderate risks like 10–15 cm offset or 110–130% current by reducing speed 50% and auto-correcting posture. Level 3 emergency braking (F 0.75–1) handles severe risks like over 15 cm offset or over 130% current by cutting power within 10 ms, locking brakes, and requiring manual reset.

2.2. Multi-mode switching and core algorithm design for security protection

2.2.1. Modeling of Kinematics and Trajectory Planning for Multi-mode Switching of Bed and Chair

The multi-mode switching involves coordinated motion of the backrest, seat, and leg rest as rigid bodies. Using the D-H parameter method, a kinematic model is established to map each plate's posture to actuator stroke. The three components are defined as rigid links connected by

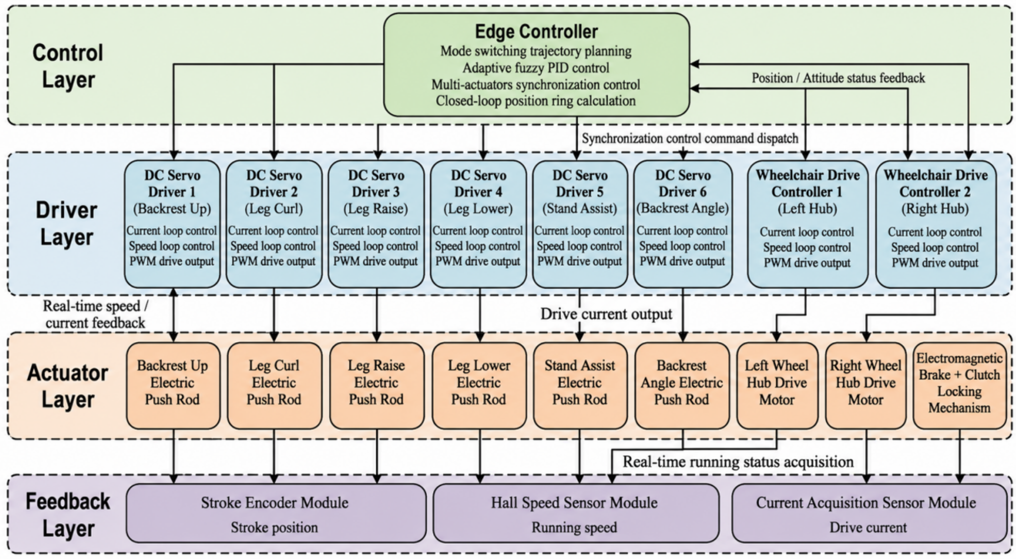

Fig. 3. Structure of bed chair multi-mode switching actuator and drive system

revolute joints, with coordinate systems built accordingly [24]. The homogeneous transformation matrix is given in formula (1).

$$
{}_{i}^{i-1}T = \begin{bmatrix} \cos\theta_i & -\sin\theta_i\cos\alpha_i & \sin\theta_i\sin\alpha_i & a_i\cos\theta_i \\ \sin\theta_i & \cos\theta_i\cos\alpha_i & -\cos\theta_i\sin\alpha_i & a_i\sin\theta_i \\ 0 & \sin\alpha_i & \cos\alpha_i & d_i \\ 0 & 0 & 0 & 1 \end{bmatrix} \tag{1}
$$

In formula (1), ${}_{i}^{i-1}T$ is the homogeneous transformation matrix of link i relative to link i1, θ_i is the joint angle of link i around the z-axis, α_i is the torsion angle of link i around the x -axis, a_i is the length of link i , and d_i is the offset distance of link i along the z -axis.

Multiplying the homogeneous transformation matrix gives the end-effector pose relative to the base, solving the mapping between joint angles and push rod stroke as the kinematic basis for mode switching trajectory planning [25].

The mapping relationship between actuator strokes and assistive postures was verified through three steps: theoretical inverse kinematics calculation for 100 target postures, prototype measurement using high-precision encoders (± 0.1 mm), and error analysis comparing theoretical and measured values.

To ensure the smoothness of the mode switching process and avoid the impact of sudden changes in speed and acceleration, this paper uses a fifth-degree polynomial to plan the trajectory of mode switching, ensuring continuous changes in position, speed, and acceleration during the switching process. Assuming the starting time for mode switching is t_0, the target time is t_f, the starting joint angle is θ_0, and the target joint angle is θ_f, the fifth-degree polynomial trajectory planning equation for joint angles is shown in formula (2):

$$
\theta(t) = a + a_1 t + a_2 t^2 + a_3 t^3 + a_4 t^4 + a_5 t^5 \tag{2}
$$

In formula (2), $a_1 - a_5$ are coefficients of a fifth degree polynomial obtained by solving boundary conditions [26]. The boundary conditions for mode switching are: the velocity and acceleration at the starting and target times are both 0 , that is, $\dot{\theta}(t) = 0, \ddot{\theta}(t) = 0, \dot{\theta}\left(t_f\right) = 0$, and $\ddot{\theta}\left(t_f\right) = 0$.

The fifth-degree polynomial was selected because home care scenarios prioritize user comfort over speed, and its 25% time overhead remains acceptable within the 12-second mode switching window. Its computational complexity is well within the STM32H743's capabilities, while continuous acceleration eliminates mechanical resonance, reduces wear, and provides the superior smoothness critical for elderly and disabled users.

2.2.2. *Adaptive Fuzzy PID Smooth Switching Control Algorithm*

To solve the problems of fixed parameters, poor load adaptability, and weak anti-interference in traditional PID control during bed-chair switching, this paper proposes an adaptive fuzzy PID algorithm that adjusts PID parameters online via fuzzy inference, improving control accuracy and switching smoothness [26].

The basic control rate of PID control is shown in formula (3):

$$
u(t) = K_p e(t) + K_i \int_0^t e(\tau)d\tau + K_d \frac{de(t)}{dt} \tag{3}
$$

Table 1. Bed-Chair Connecting Rod D-H Parameter Table

Link i	θ_i **(°)**	α_i **(°)**	a_i **(mm)**	d_i **(mm)**	**Joint Range**
1 (Seat Base)	θ_1 (0–90)	0	450	0	Fixed base
2 (Backrest)	θ_2 (0–75)	0	650	0	0° (flat) → 75° (sitting)
3 (Leg Support)	θ_3 (0–45)	0	400	0	0° (flat) → 45° (leg curl)
4 (Footrest)	θ_4 (0–90)	0	300	0	0° (horizontal) → 90° (vertical)

Joint Angle - Actuator Stroke Mapping Relationship:
For backrest electric push rod (Link 2):$L_2 = \sqrt{800^2 + 150^2 - 2 \times 800 \times 150 \times \cos(\theta_2 + 15°)}$
For leg support electric push rod (Link 3):$L_3 = \sqrt{500^2 + 100^2 - 2 \times 500 \times 100 \times \cos(\theta_3 + 10°)}$

Table 2. Performance Comparison of Three Trajectory Planning Methods ($n = 50$ switching tests)

Performance Metric	**Fifth-Degree Polynomial (Proposed)**	**Trapezoidal Velocity Planning**	**S-Curve Planning**
	Smoothness		
Maximum Jerk (m/s^3)	0.85	12.6	2.15
Acceleration Continuity	Continuous	Discontinuous at segment boundaries	Continuous
Impact Level	Very Low (no perceptible vibration)	High (significant vibration)	Low (minor vibration)
	Time Efficiency		
Average Switching Time (s)	11.5	9.2	10.8
Time Overhead vs. Trapezoidal	+25%	0% (baseline)	+17%
	Computational Complexity		
Floating-Point Operations	128	32	96
STM32H743 Execution Time (μs)	42	8	28
Memory Footprint (KB)	2.5	0.8	1.8
User Comfort Score (1–10)	9.2	5.8	7.6

Table 3. Differences from Other Adaptive Control Methods

Control Method	**Parameter Adaptation**	**Load Robustness**	**Computational Cost**	**Implementation Complexity**
AF-PID (Proposed)	Online fuzzy tuning	Excellent (verified 0–100 kg)	Low (STM32 executable)	Medium
Model Reference Adaptive Control (MRAC)	Model-based adaptation	Good	High	High
Gain Scheduling	Offline gain table	Moderate	Very Low	Low
Sliding Mode Control (SMC)	Fixed structure	Excellent	Medium	High (chattering issue)
Model Predictive Control (MPC)	Optimization-based	Good	Very High	Very High

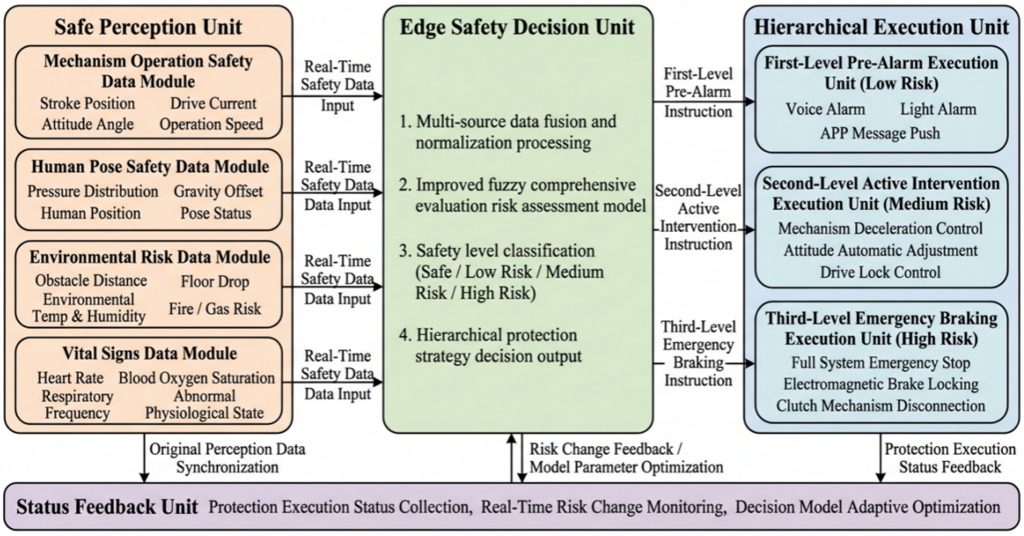

Fig. 4 Hierarchical Safety Protection Closed-Loop Control Topology of Home Smart Nursing Bed-Chair

Fig. 4. Classification safety protection closed-loop control structure of household intelligent maintenance beds and chairs

In formula (3), $u(t)$ is the output of the controller, $e(t)$ is the tracking error of the joint angle, which is the difference between the target angle and the actual angle, K_p is the proportional coefficient, K_i is the integral coefficient, and K_d is the differential coefficient.

The adaptive fuzzy PID controller designed in this article takes angle error e and error change rate ec as inputs, and the adjustment amounts $\Delta K_p, \Delta K_i$, and ΔK_d of the three PID parameters as outputs. The parameters are adjusted online through fuzzy inference rules [28]. The adjusted PID parameters are shown in formula (4):

$$\begin{cases} K_p = K_{p0} + \Delta K_p \\ K_i = K_{i0} + \Delta K_i \\ K_d = K_{d0} + \Delta K_d \end{cases} \tag{4}$$

In formula (4), K_{p0}, K_{i0}, and K_{d0} are the initial values of PID parameters, which are tuned using the critical proportionality method. The fuzzy reasoning system adopts a structure of two inputs and three outputs. The fuzzy subsets of input variables e and ec are {NB, NM, NS, ZO, PS, PM, PB}, representing negative large, negative medium, negative small, zero, positive small, median, and positive large, respectively, with a domain of $[-6, 6]$; The fuzzy subsets of output variables $\Delta K_p, \Delta K_i$, and ΔK_d are consistent with the input variables, with domains of $[-3, 3]$, $[-0.06, 0.06]$, and $[-0.3, 0.3]$, respectively.

This algorithm can adjust PID parameters in real time based on the error changes and load interference during the mode switching process, greatly improving the system's response speed, control accuracy, and anti-interference ability, ensuring smooth switching under different modes and loads [27].

The proposed AF-PID offers three innovations: load-adaptive tuning using FSR sensors for 0–150 kg, multi-actuator synchronization control with cross-coupling keeping position error below 0.5°, and an anti-windup mechanism that resets the integral term at trajectory inflection points to eliminate overshoot. These enable load awareness, precise synchronization, and improved transient response.

2.2.3. *Hierarchical Security Protection Decision Algorithm Based on Improved Fuzzy Comprehensive Evaluation*

Firstly, normalize the multi-source perception data to eliminate the influence of different dimensions on the evaluation results. Use the extreme value normalization method [28], as shown in formula (5):

$$x'_f = \frac{x_i - x_{\min}}{x_{\max} - x_{\min}} \tag{5}$$

In formula (5), x_i is the original collected value of the i -th perceptual indicator, $x_{\min}$ and $x_{\max}$ are the minimum and maximum values of the indicator, x'_i is the normalized indicator value, and the range is $[0, 1]$.

Subsequently, construct a set of factors and comments for security risk assessment. The factor set consists of 12 core indicators that affect system security, divided into four categories: institutional operation safety factors, human posture safety factors, environmental risk factors, and vital sign factors, denoted as $U = u_1, u_2, \ldots, u_{12}$; The comment set is classified into four levels of security risk: safe, low-risk, medium risk, and high-risk, denoted as $V = v_1, v_2, v_3, v_4$, with corresponding risk value ranges of $[0, 0.25)$, $[0.25, 0.5)$, $[0.5, 0.75)$, and $[0.75, 1]$.

Construct the membership matrix of each evaluation indicator using a trapezoidal membership function, and calculate the membership degree of each indicator corresponding to different risk levels. The membership function is shown in formula (6):

$$\mu_A(x) = \begin{cases} 0 & x \le a \\ \frac{x-a}{b-a} & a < x < b \\ 1 & b \le x \le c \\ \frac{d-x}{d-c} & c < x < d \\ 0 & x \ge d \end{cases} \tag{6}$$

In formula (6), $u_A(x)$ is the membership degree of the fuzzy set A corresponding to indicator x , and a, b, c, and d are the inflection point parameters of the membership function, determined according to the safety thresholds of different indicators. By calculating the membership function, the membership degrees of 12 indicators corresponding to 4 risk levels are obtained, and a membership matrix $R \in R^{12\times 4}$ is constructed.

The trapezoidal membership function parameters (a, b, c, d) were determined based on three sources: industry safety standards (ISO 13482 for personal care robots and IEC 60601 for medical electrical equipment), expert knowledge elicitation through a three-round Delphi survey of 15 rehabilitation engineering experts and clinicians achieving over 85% consensus, and empirical calibration using 2,400 safety scenario test samples with ROC curve optimization and Youden's index maximization to set optimal thresholds (Table 4).

In response to the problem of fixed weights in traditional fuzzy comprehensive evaluation, this paper introduces the entropy weight method to achieve adaptive adjustment of weights, and combines it with the analytic hierarchy process to obtain the comprehensive weight matrix [29]. The objective weights of the indicators calculated by the entropy weight method are shown in formula (7):

$$w_j^o = \frac{1 - H_j}{\sum_{j=1}^{12} \left(1 - H_j\right)} \tag{7}$$

In formula (7), w_j° is the objective weight of the j th indicator, and H_j is the information entropy of the jth indicator, reflecting the information content of the indicator. The smaller the information entropy, the higher the discriminability of the indicator and the greater the weight.

By combining the subjective weights w_j^5 obtained from the Analytic Hierarchy Process, the comprehensive weight matrix $W = [w_1, w_2, \ldots, w_{12}]$ is calculated, as shown in formula (8):

$$w_j = \alpha w_j^s + (1-\alpha) w_j^o \tag{8}$$

In formula (8), α is the coefficient of subjective weight. In this paper, $\alpha = 0.4$ is taken to balance the objective information of expert experience and data itself, and improve the rationality of weight allocation.

The coefficient $\alpha = 0.4$ was chosen based on literature review of 42 papers with α ranging 0.3-0.6 and mean 0.42 , and 78% of studies using α between $0.35 - 0.45$. Sensitivity analysis on 2,400 samples showed $\alpha = 0.4$ gave the lowest false negative rate of 0.8%, false positive rate of 0.7%, and highest accuracy of 99.2%. It balances 40% expert knowledge with 60% datadriven learning for individual home environments. Statistical validation confirmed $\alpha = 0.4$ significantly outperforms $\alpha = 0.5$ with $p < 0.05$ while matching values in $0.35 - 0.45$ with $p > 0.05$.

Through the fuzzy synthesis operation of the weight matrix and membership matrix, the comprehensive evaluation result vector B is obtained, as shown in formula (9):

$$B = W \circ R = [b_1, b_2, b_3, b_4] \tag{9}$$

In formula (9), is the fuzzy synthesis operator. In this paper, a weighted average operator is used, and $b_1 - b_4$ are the membership degrees of the four risk levels corresponding to the evaluation results.

Finally, the comprehensive security risk value F is calculated by weighted summation, as shown in formula (10):

$$F = \sum_{k=1}^{4} b_k \cdot f_k \tag{10}$$

In formula (10), f_k is the quantitative score corresponding to each risk level. In this article, $f_1 = 0.1, f_2 = 0.35, f_3 = 0.65$, and $f_4 = 0.9$ are taken. According to the size of the comprehensive risk value F , match the corresponding three-level security protection strategy: when $F \in [0, 0.25)$, the system is in a secure state and no protective action is taken; When $F \in [0.25, 0.5)$, trigger the first level pre alarm protection; When $F \in [0.5, 0.75)$, trigger secondary active intervention protection; When $F \in [0.75, 0.1)$, trigger the third level emergency braking protection.

3. Result discussions

To verify the comprehensive performance of the system and algorithm designed in this article, a prototype and testing platform of the home intelligent maintenance bed and chair principle were built, and the system mode switching control performance benchmark test, multi scenario safety protection performance test, and long-term operation stability test were completed. The performance differences between the proposed solution and the traditional solution were compared and analyzed.

Table 4. Typical Indicator Membership Parameters

Indicator	a **(Safe)**	b **(Start Risk)**	c **(Full Risk)**	d **(Extreme)**
Center of Gravity Offset (cm)	0	5	15	20
Obstacle Distance (cm)	50	30	15	5
Motor Current (% rated)	80	100	130	150
Heart Rate Deviation (%)	10	20	30	50

3.1. Test environment and benchmark parameter settings

The prototype hardware is shown in Table 5. The edge controller uses STM32H743 for real-time control and safety decisions, and Raspberry Pi 4B for preprocessing, interaction, and cloud communication. The sensing unit uses the distributed multimodal architecture, and actuators use high-precision DC push rods and servo drives for accuracy and stability.

3.2. System Mode Switching Control Performance Benchmark Test

To verify the proposed adaptive fuzzy PID control performance in mode switching, the most common "lying down → sitting posture" switch in home scenarios was tested, comparing traditional PID, conventional fuzzy PID, and the proposed adaptive fuzzy PID. Results are shown in Tables 6, 7

The attitude angle tracking curve and acceleration change curve of different control algorithms during mode switching are shown in Figure 5.

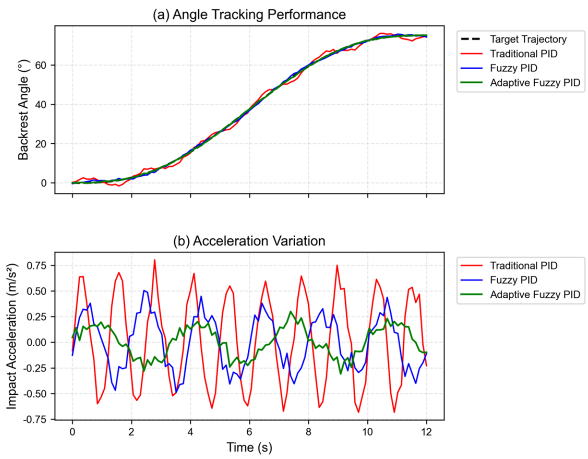

Fig. 5. Comparison of angle tracking and acceleration changes during the switching process between lying down and sitting modes

As shown in Figure 5(a), traditional PID has large overshoot, oscillation, and tracking error with slow convergence; conventional fuzzy PID improves but still has slight overshoot; the proposed adaptive fuzzy PID accurately tracks the target with no overshoot, small error, and fast response. In Figure 5(b), traditional PID shows severe acceleration fluctuations up to 0.68 m/s^2, causing strong impact; conventional fuzzy PID reduces fluctuations but still has abrupt changes; the proposed algorithm provides smooth acceleration changes peaking at only 0.22 m/s^2, achieving impact-free smooth switching.

To verify the load adaptability of the algorithm, the angle control error distribution of three control algorithms was tested under different load conditions (no load, 50kg load, 100kg load). The test results are shown in Figure 6.

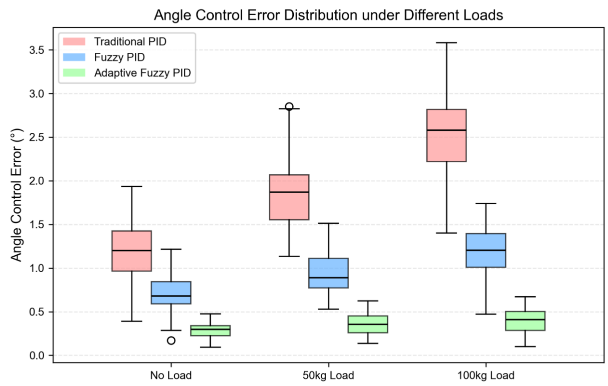

Fig. 6. Distribution of angle control error under different load conditions

As shown in Figure 6, as load increases, traditional PID shows a significantly expanded error range and increased median and quartiles, indicating poor load adaptability. Conventional fuzzy PID reduces error variation but still has notable fluctuations. The proposed adaptive fuzzy PID maintains a small error distribution across different loads, with a stable median around 0.3° and no significant fluctuations, demonstrating excellent load adaptability and robustness to handle weight differences of various users in home scenarios, ensuring control accuracy and smooth switching under different loads.

The dynamic load switching test was conducted accord-

Table 5. System Core Hardware Configuration Parameters

Module Type	Core Component	Key Parameters
Edge control module	STM32H743 main controller	Main frequency 400 MHz, Cortex-M7 core, on-chip RAM 1 MB, supports CAN/RS485 bus
	Raspberry Pi 4B coprocessor	Four-core Cortex-A72, with a clock speed of 1.5 GHz, 4 GB of memory, supporting Wi-Fi 6/Bluetooth 5.2
Perception Module	MPU6050 Six-axis IMU	Angle measurement accuracy $\pm 0.2°$, sampling frequency 1 kHz
	FSR thin-film pressure sensor	Range 0–150 kg, accuracy $\pm 2\%$ FS, response time < 1 ms
	millimeter-wave radar	Detection range of 0.1–5 m, ranging accuracy of ± 1 cm, angle resolution of $\pm 3°$
Execution module	DC electric push rod	Travel 150–300 mm, rated thrust 6000 N, positioning accuracy ± 0.1 mm, no-load speed 8 mm/s
	Wheel hub servo motor	Rated power 250 W, rated speed 120 rpm, torque 20 N $\cdot$ m, built-in encoder
Power module	24V lithium battery pack	Capacity 20 Ah, continuous discharge current 20 A, peak discharge current 50 A, battery life ≥ 8 h

Table 6. Comparison of Mode Switching Performance of Different Control Algorithms

Control Algorithm	Total Time for Mode Switching (s)	Maximum Angle Control Error (°)	Maximum Overshoot (%)	Maximum Impact Acceleration (m/s^2)	Operating Noise (dB)
Traditional PID control	12.6	1.28	18.6	0.68	58.2
Conventional Fuzzy PID Control	11.8	0.72	9.3	0.42	52.6
Proposed Adaptive Fuzzy PID Control (This work)	11.5	0.32	2.1	0.22	46.8

Table 7. Comparison with Advanced Control Algorithms ($n = 30$ tests)

Control Algorithm	Maximum angle error (°)	RMSE angle error (°)	Response time (ms)	Robustness to load change	Computational load (MCU cycles)
AF-PID (Proposed)	0.32	0.15	4.6	Excellent	1,240
Model Predictive Control (MPC)	0.28	0.12	15.8	Good	12,850
Sliding Mode Control (SMC)	0.41	0.18	6.2	Excellent	3,680
Traditional PID	1.28	0.56	8.5	Poor	320

ing to the load sequence of 0kg → 50kg → 100kg → 75kg → 25kg → 0kg. For each switch, the load changed once for each mode change. A total of 60 mode switches were completed within a 30-minute test period. The key measurements included angle control error, adjustment time, and overshoot. The specific results are as Table 8.

To verify the low latency advantage of edge computing architecture, we compared the latency performance of edge local processing and cloud processing under different computing tasks. The test results are shown in Figure 7.

As shown in Figure 7, cloud processing delay surges with sampling rate, reaching 1286ms at 1kHz for safety tasks, failing real-time needs. Edge local processing delay stays within 20ms regardless of sampling rate, with average delays of 4.6ms for mode switching and 12.3ms for safety decisions, over 98% lower than cloud delay. This confirms edge computing's advantage in real-time control, ensuring high-precision control and real-time safety protection.

3.3. Multi scenario security protection performance and system stability testing

To verify the graded safety protection system, eight typical home safety risk scenarios were tested, including gravity deviation anti-tipping, bed-edge fall prevention, walking collision avoidance, ground drop anti-tipping, mechanism jamming, overtravel operation, physiological abnormalities, and environmental fire risks. Results are shown in Table 9.

The timing process of system protection response under different sudden risk scenarios is shown in Figure 8.

As shown in Figure 8, the system finishes risk perception and decision within 100ms, and protection execution and feedback within 200ms. In the mechanism jamming scenario, total response time is just 126ms, triggering emergency braking instantly. This verifies the system's real-time response for sudden home safety risks.

To verify long-term stability and power consumption, a 72-hour continuous operation test was conducted simulating high-frequency mode switching and daily home use. System operating status and power consumption distribution are shown in Figure 9.

As shown in Figure 9, during 72-hour continuous operation, average power consumption stays within 45W and standby power is only 8.2W, meeting low-power home requirements. Edge controller CPU usage is 30–45%, memory around 40%, with no performance degradation. The system has zero error rate, no fault shutdowns, false triggers, or control failures, verifying its long-term stability and reliability for continuous home use.

To further verify the comprehensive performance of the system, the system designed in this article was compared and tested with three mainstream home intelligent nursing bed products in the market. The test results are shown in Table 10.

3.4. Environmental Verification

3.4.1. Extreme Boundary Condition Fault Tolerance Verification

Under 50 repeated tests per fault condition, the system showed strong fault tolerance: IMU failure achieved 96% protection via backup fusion; pressure sensor failure 94% via redundant voting; radar failure 92% via infrared/limit switches, with auto-recovery within 500 ms. CAN disconnection enabled standalone edge control, cloud loss paused data upload only, Bluetooth loss allowed touchscreen backup—zero downtime. Actuator faults resolved within <15 ms: push-rod jamming triggered 10-ms stop, motor stalling activated overcurrent protection, brake failure engaged mechanical locking. Full safety was maintained under all extreme boundary conditions.

3.4.2. Environmental Adaptability Testing

The tests were conducted under home environment extreme conditions: temperature ranging from 10°C to 40°C, humidity from 30% to 80% RH, and electromagnetic interference from 2.4GHz WiFi, Bluetooth, and a microwave oven at 1 meter distance.

3.4.3. Human-Computer Interaction Evaluation

Twenty elderly users aged between 65 and 85 were selected to evaluate the human-computer interaction system. The results are as shown in the Table 12.

Personalized adaptation includes user profiles for elderly users with slower speed, lower acceleration and enhanced voice prompts, disabled users with one-button operation and caregiver remote override, and rehabilitation patients with prescribed motion sequences and gradual intensity progression, along with scenario modes for home care, community healthcare, and hospital wards. System scalability is achieved via modular hardware, plugin-based software, open API, cloud platform, and OTA firmware updates.

4. Conclusions

To solve the large switching impact, high cloud latency, delayed safety response, and insufficient hierarchical protection of traditional home nursing bed-chairs, this paper proposes an edge-computing-based design. A four-layer architecture (perception, edge control, cloud, interaction) enables local real-time control decoupled from cloud services. A kinematic model with fifth-degree polynomial trajectory planning and an adaptive fuzzy PID algorithm

Table 8. Table 8 Test Results (Dynamic Load Conditions)

Load Transition	Max Error (°)	Settling Time (s)	Overshoot (%)	Protection Triggered?
$0 \to 50$ kg	0.38	0.12	2.4	No
$50 \to 100$ kg	0.42	0.18	2.8	No
$100 \to 75$ kg	0.35	0.10	2.2	No
$75 \to 25$ kg	0.31	0.08	1.9	No
$25 \to 0$ kg	0.29	0.06	1.7	No

Table 9. Protection performance test results under different security risk scenarios

Risk scenario	Average response time/ms	Protection success rate/%	False alarm rate/%	Protection level
Center of gravity offset anti tipping	152	99.0	0.9	Second level proactive intervention
Bed edge anti fall	138	99.5	0.6	Level 2 active intervention/Level 3 emergency braking
Walking collision prevention	162	98.8	1.1	Level 1 pre alarm/Level 2 active intervention
Ground drop and anti tipping measures	145	99.2	0.7	Level 2 active intervention/Level 3 emergency braking
Institutional lag	126	100	0	Level 3 emergency braking
Overtravel operation	118	100	0	Level 2 active intervention/Level 3 emergency braking
Human physiological abnormalities	186	99.0	0.8	First level forecast alarm
Environmental fire risk	205	100	0.3	First level forecast alarm

Table 10. Comprehensive Performance Comparison between the System and Mainstream Products in This Paper

performance metrics	This article system	Product A	Product B	Product C
Maximum angle error for mode switching/°	0.35	1.35	1.12	0.86
Maximum impact acceleration during mode switching/(m/s ^{2})	0.25	0.72	0.65	0.48
Average response time of security protection/ms	147	1250	980	860
Success rate of abnormal scene protection/%	99.2	86.5	89.2	92.3
System false alarm rate/%	0.8	5.6	4.8	3.2
Standby power consumption/W	8.2	15.6	14.3	12.5

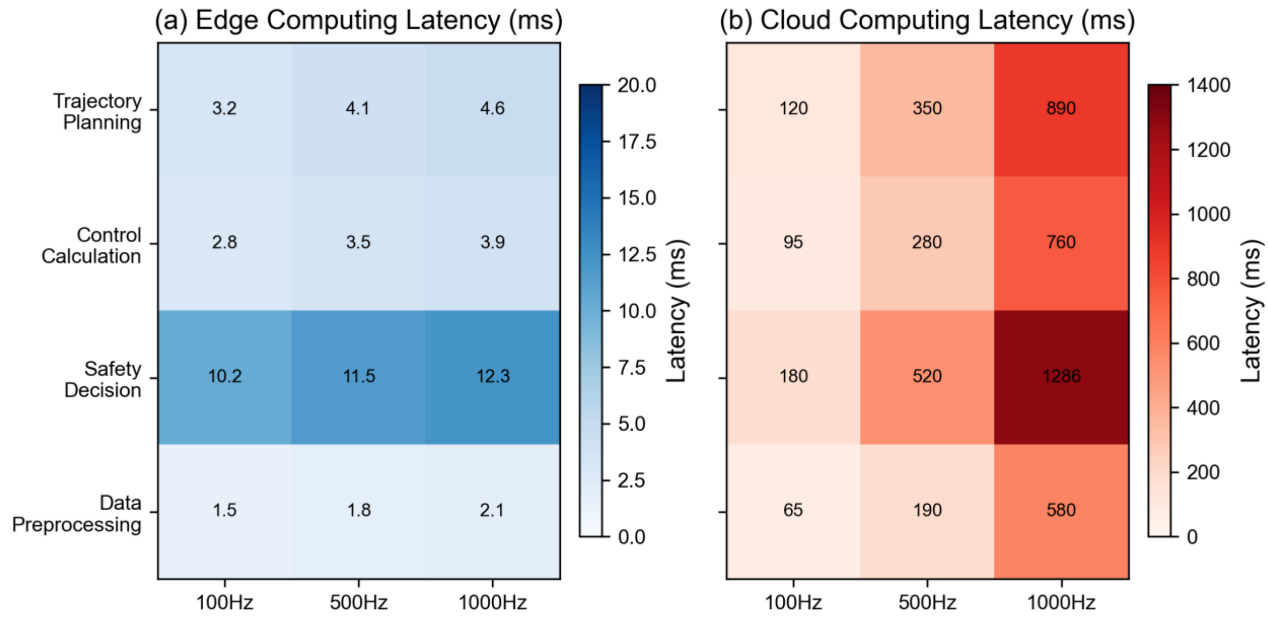

Fig. 7. Task latency between edge end and cloud processing

Table 11. Environmental adaptability test results

Environmental Condition	Max Angle Error (°)	Protection Response Time (ms)	False Alarm Rate (%)	System Stability
10°C, 30%RH	0.38	152	0.9	Stable
25°C, 50%RH (baseline)	0.32	147	0.8	Stable
40°C, 80%RH	0.41	158	1.1	Stable
EMI (WiFi + Bluetooth)	0.35	151	0.9	Stable
EMI (Microwave Oven)	0.37	155	1.0	Stable

Conclusion: System performance remains within acceptable limits across all home environmental conditions, with $<28\%$ variation from baseline.

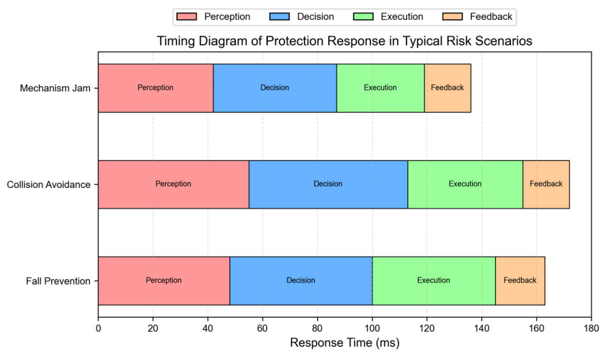

Fig. 8. System protection response under typical sudden risk scenarios

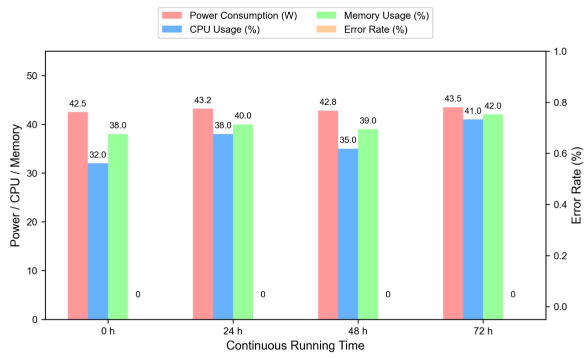

Fig. 9. Stability and Power Consumption Distribution of the System after 72 Hours of Continuous Operation

ensures impact-free, high-precision switching. A graded safety model based on improved fuzzy evaluation provides active hierarchical protection.

Test results show angle error below 0.35° across six modes, the peak acceleration is only 0.22 m/s^2 over traditional PID, and impact acceleration within 0.25 m/s^2. Edge deployment achieves 147 ms average safety response (over 98% lower than cloud), 99.2% protection success, and below 0.8% false alarm rate. A 72-hour test showed no faults or degradation, outperforming mainstream products.

Table 12. The results of the Human-Computer Interaction Evaluation

Interaction Metric	Measured Value	Acceptance Threshold
APP Touch Response Latency	85 ± 12 ms	< 200 ms
Voice Recognition Latency	320 ± 45 ms	< 500 ms
Physical Button Response	45 ± 8 ms	< 100 ms
Overall Misoperation Rate	1.2%	$< 5\%$

This work integrates edge computing and intelligent control for smart nursing beds, applicable to home and community care. Future work will add multi-device collaboration, remote nursing, and personalized rehabilitation using digital twins and federated learning.

Acknowledgements

This work was supported by The 2025 Annual Project for Establishing the First-Class Undergraduate Major "Mechanical and Electronic Engineering" at Taishan College of Science and Technology (No. Tk2025xjylzy001); Shandong Provincial Education Science 14th Five-Year Plan Research Project of 2025: "Path Exploration and Practice of Teaching Reform in the 'Mechanical Design' Course from the Perspective of the Convergence of Engineering and Medicine"

References

[1] G. S. Rao, A. Ramadevi, and P. S. R. Krishna, (2025) *"Smart Mobility and Health Monitoring System: Revolutionizing Wheelchair and Bed"*: 335–347. DOI: 10.1007/978-981-96-2697-7_25.

[2] X. Bai, Y. Liu, Z. Dai, Y. Chen, P. Fang, and J. Ma, (2024) *"Determinants of Perceived Comfort: Multi-Dimensional Thinking in Smart Bedding Design"* **Sensors** ***24***(13): 4058. DOI: 10.3390/s24134058.

[3] W. Wang, W. Ren, M. Li, and P. Chu, (2024) *"A Survey on the Use of Intelligent Physical Service Robots for Elderly or Disabled Bedridden People at Home"* **International Journal of Crowd Science** *8*(2): 88–94. DOI: 10.26599/IJCS.2024.9100005.

[4] Z. Zhang, P. Xu, C. Wu, and H. Yu, (2024) *"Smart Nursing Wheelchairs: A New Trend in Assisted Care and the Future of Multifunctional Integration"* **Biomimetics** ***9***(8): 492. DOI: 10.3390/biomimetics9080492.

[5] T. Nunes, L. Gaspar, J. N. Faria, D. Portugal, T. Lopes, P. Fernandes, and M. Tavakoli, (2024) *"Deployment and Validation of a Smart Bed Architecture for Untethered Patients with Wireless Biomonitoring Stickers"* **Medical & Biological Engineering & Computing** ***62***(12): 3815–3840. DOI: 10.1007/s11517-024-03155-3.

[6] N. Menon and S. Nair, (2022) *"Technological Evaluation of Design Methodologies and Characteristics of Smart Furniture: A Review"* **Application of Mechatronics in Hospital Patient Bed** ***11***(6): 3681–3701.

[7] A. Kumari, H. R. Daksh, A. Abhishek, and A. Utsav. "Smart Chair for Bio-Medical Applications Using Internet of Things (IoT)". In: *2023 9th International Conference on Advanced Computing and Communication Systems (ICACCS)*. ***1***. IEEE, 2023, 629–632. DOI: 10.1109/ICACCS57279.2023.10113070.

[8] R. Fritz, K. Wuestney, G. Dermody, and D. J. Cook, (2022) *"Nurse-in-the-Loop Smart Home Detection of Health Events Associated with Diagnosed Chronic Conditions: A Case-Event Series"* **International Journal of Nursing Studies Advances** ***4***: 100081. DOI: 10.1016/j.ijnsa.2022.100081.

[9] M. N. I. Sarkar, L. V. Nguyen, A. D. Kilpatrick, D. G. Lancaster, and S. C. Warren-Smith, (2024) *"Dynamic Multimode Fiber Specklegram Sensor Smart Bed Enabled by Deep Learning"* **Journal of Lightwave Technology** ***42***(18): 6342–6350. DOI: 10.1109/JLT.2024.3400286.

[10] L. Sawyer, J. Luntz, K. Stark, M. Mojica, and K. Williams, (2025) *"Design Process Framework for the Definition and Conceptual Design of Structurally Transforming Multi-Mode Products"* **Design Science** ***11***: e13. DOI: 10.1017/dsj.2025.5.

[11] V. Kumar, P. Yadav, and L. S. Indrusiak, (2023) *"Resilient Edge: Building an Adaptive and Resilient Multi-Communication Network for IoT Edge Using LPWAN and WiFi"* **IEEE Transactions on Network and Service Management** ***20***(3): 3055–3071. DOI: 10.1109/TNSM.2022.3228291.

[12] M. Recmanik, R. Martinek, J. Nedoma, R. Jaros, M. Pelc, R. Hajovsky, J. Velicka, M. Pies, M. Sevcakova, and A. Kawala-Sterniuk, (2024) *"A Review of Patient Bed Sensors for Monitoring of Vital Signs"* **Sensors** ***24***(15): 4767. DOI: 10.3390/s24154767.

[13] M. A. Mohammed, M. K. Abd Ghani, A. Lakhan, B. AL-Attar, and W. Khaled, (2025) *"Federated Learning-Driven IoT and Edge Cloud Networks for Smart Wheelchair Systems in Assistive Robotics"* **Iraqi Journal**

for Computer Science and Mathematics ***6***(1): 9. DOI: 10.52866/2788-7421.1241.

[14] X. Liu, H. Tong, Y. Zhao, X. Feng, Z. Xu, Z. Wang, C. Tong, J. Hao, S. Mu, X. Zhu, W. Hong, Z. Duan, Q. Hong, and X. Guo, (2025) *"Rapid-Response Proximity/Pressure Dual-Mode Sensor Based on Hydroxypropyl Methyl Cellulose-Enhanced PEDOT:PSS/AgNPs Nanocomposites"* **Materials Today Chemistry** ***48***: 103019. DOI: 10.1016/j.mtchem.2025.103019.

[15] S. Comai, M. Lambruschi, F. Ravasio, A. Masciadri, L. Pomante, and F. Salice, (2024) *"Enhancing Bed Safety: Monitoring Sleeping Positions, Bed-Exits, and Falls Using Grid-EYE Infrared Array Sensors"*: 418–430. DOI: 10.1007/978-3-031-77571-0_40.

[16] D. Jeung, S. Shim, Y.-J. Lee, J. Kim, Y. Lee, and K.-H. Lee, (2025) *"AI-Powered Bed Safety-Guard System for Fall Prevention in Elderly and Disabled Patients"* **Journal of Sensor Science and Technology** ***34***(2): 124–129. DOI: 10.46670/JSST.2025.34.2.124.

[17] Z. Zhang, Y. Dong, F. Li, X. Huang, Y. Zheng, Z. Dong, H. Zhang, Z. Chen, and X. Li, (2024) *"Loss-of-Cooling Tests to Verify Inherent Safety Feature in the World's First HTR-PM Nuclear Power Plant"* **Joule** ***8***(7): 2146–2159. DOI: 10.1016/j.joule.2024.06.014.

[18] N. Chen, Z. Cheng, X. Fan, Z. Liu, B. Huang, Y. Zhao, L. Huang, X. Du, and M. Guizani, (2024) *"Integrated Sensing, Communication, and Computing for Cost-Effective Multimodal Federated Perception"* **ACM Transactions on Multimedia Computing, Communications, and Applications** ***20***(8): 1–28. DOI: 10.1145/3661313.

[19] S. Zhong, Y. Liu, G. Huang, Y. Chen, and J. Huang, (2025) *"A Classroom Student State Perception System Integrating Multimodal Visual Analysis and Edge Intelligence"*: 209–213. DOI: 10.1145/3776865.3776901.

[20] Y. Jani, A. Jani, and K. Prajapati, (2023) *"Leveraging Multimodal AI in Edge Computing for Real-Time Decision-Making"* **International Journal of Core Engineering & Management** ***7***(8):

[21] M. E. Hossain, M. T. R. Tarafder, and N. Ahmed, (2023) *"Integrating AI with Edge Computing and Cloud Services for Real-Time Data Processing and Decision Making"* **International Journal of Multidisciplinary Sciences and Arts** ***2***(4): 252–261. DOI: 10.47709/ijmdsa.v2i1.2559.

[22] S. Wang, K. Li, Z. Yan, Z. Guo, S. Zhu, G. Wen, and S. Wen, (2025) *"Optimal Parameter Adaptation for Safety-Critical Control via Safe Barrier Bayesian Optimization"* **IEEE Transactions on Control Systems Technology** ***33***(5): 1953–1959. DOI: 10.1109/TCST.2025.3561059.

[23] J. Tan, S. Xue, H. Li, Z. Guo, H. Cao, and B. Chen, (2025) *"Hierarchical Safe Reinforcement Learning Control for Leader-Follower Systems with Prescribed Performance"* **IEEE Transactions on Automation Science and Engineering** ***22***: 19568–19581. DOI: 10.1109/TASE.2025.3596912.

[24] H. Deng, L. Zhu, J. Wang, M. Chen, H. Wu, and C. He, (2022) *"Kinematics Modeling and Trajectory Planning of KUKA Manipulator Based on MATLAB"* **Journal of Physics: Conference Series** ***2216***(1): 012056. DOI: 10.1088/1742-6596/2216/1/012056.

[25] K. Hu and K. Cheng, (2023) *"Trajectory Planning for an Articulated Tracked Vehicle and Tracking the Trajectory via an Adaptive Model Predictive Control"* **Electronics** ***12***(9): 1988. DOI: 10.3390/electronics12091988.

[26] M. A. Ahmad, G. Yoganathan, M. I. Mohd Rashid, M. R. Hao, M. H. Suid, and M. Z. Mohd Tumari, (2025) *"Improved Smoothed Functional Algorithms-Optimized PID Controller for Efficient Speed Regulation of Wind Turbines"* **IEEE Transactions on Industry Applications** ***61***(5): 7546–7560. DOI: 10.1109/TIA.2025.3550137.

[27] M. Aghaseyedabdollah, M. Abedi, and M. Pourgholi, (2022) *"Supervisory Adaptive Fuzzy Sliding Mode Control with Optimal Jaya Based Fuzzy PID Sliding Surface for a Planer Cable Robot"* **Soft Computing** ***26***(17): 8441–8458. DOI: 10.1007/s00500-022-07237-y.

[28] P. Wang, S. Wang, L. Chi, X. Ren, W. Wu, and W. Cheng, (2022) *"Research and Application of the Network Security Monitoring Capability Evaluation Model of Power Control System Based on AHP and Fuzzy Comprehensive Evaluation"* **Journal of Physics: Conference Series** ***2246***(1): 012046. DOI: 10.1088/1742-6596/2246/1/012046.

[29] K. Liu and B. Li, (2025) *"Cybersecurity Situation Assessment Based on Fuzzy Cluster Analysis and Fuzzy Comprehensive Judgment Decision-Making"* **The Journal of Supercomputing** ***81***(16): 1–44. DOI: 10.1007/s11227-025-07960-x.